applied sciences

MDPI

Review

Role of Amine Type in CO_2 Separation Performance within Amine Functionalized Silica/Organosilica Membranes: A Review

Liang Yu, Masakoto Kanezashi, Hiroki Nagasawa, and Toshinori Tsuru *

Department of Chemical Engineering, Hiroshima University, 1-4-1 Kagamiyama, Higashi-Hiroshima 739-8527, Japan; liangyu@hiroshima-u.ac.jp (L.Y.); kanezashi@hiroshima-u.ac.jp (M.K.); nagasawa@hiroshima-u.ac.jp (H.N.)

* Correspondence: tsuru@hiroshima-u.ac.jp; Tel.: +81-824247714

Received: 03 June 2018; Accepted: 20 June 2018; Published: 24 June 2018

Abstract: Various types of amine-functionalized silica/organosilica membranes have been developed due to their potentially superior CO_2 separation performance. This article reviews the progress made in this field and special attention is paid to elucidating the role of amine type in CO_2 separation performance within amine-functionalized silica/organosilica membranes. This review includes a systematic comparison of various organosilica membranes with either unhindered or sterically hindered amines developed in our previous studies. Herein, we thoroughly discuss the structural characterizations and CO_2 adsorption/desorption properties of amine-functionalized xerogel powders and CO_2 transport/separation performance across the relevant membranes. Future directions for the design and development of high-performance CO_2 separation membranes are suggested, and particular attention is paid to the future of activation energies for gas permeation.

Keywords: carbon dioxide separation; organosilica membrane; amine type; sterical hindrance; activation energy for permeation

1. Introduction

The ever-increasing rate of greenhouse gas emissions in the atmosphere, particularly CO_2 generated from the combustion of fossil fuels, has led to serious global climate concerns. Therefore, efficient CO_2 capture technologies such as absorption/adsorption of CO_2 sorbents, cryogenic separation, and membrane separation, have been developed experimentally and industrially over the past few decades. Among them, membrane technology is attracting growing attention owing to its inherent advantages that include energy-efficiency, ease of operation and scale-up, and a small footprint [1–5]. As one of the most important members of the membrane family, organosilica membranes have been applied to various membrane processes with superior separation performance and a high tolerance to harsh conditions. Typical organosilica membranes developed for CO_2/N_2 separation are either microporous with rigid pores or nonporous with "free-volume" pores. Separations are therefore achieved mainly by the effect of molecular sieving along with partial contributions from selective surface diffusion through rigid pores and/or solution-diffusion within a nonporous structure. The selectivity is always less arresting due to the comparable kinetic diameters of CO_2 (3.3 Å) and N_2 (3.64 Å) and due as well to the difficulty in precisely controlling the pore (rigid or free-volume type) sizes. Given this, various amine-functionalized silica-based membranes have been developed to accomplish CO_2 separation from gas mixtures with potentially enhanced efficiency [6–13]. These membranes are expected to show great potential in simultaneously promoting CO_2 permeance and permselectivity due to the reversible reactions between CO_2 and amine groups. Thus

far, however, only a limited number of membranes have offered appealing CO_2 separation performance with both high CO_2 permeance and CO_2/gas permselectivity irrespective of many reports of amine-functionalized silica-based membranes. Instead, in some cases even reverse CO_2/N_2 selectivity under a dry state has been observed [13]. Whereas, in some cases, other types of membranes with only CO_2-philic groups rather than chemical reactions, such as poly(ethylene oxide)-based membranes, have resulted in attractive CO_2 separation performance [2]. Hence, further fundamental studies in terms of the effect of amine-CO_2 chemical interactions on CO_2 transport behaviors through amine-functionalized silica-based membranes are needed to direct the fabrication of high-performance CO_2 separation membranes.

In general, how fast and selectively the species to be separated can enter into, transport through, and exit from the membrane govern the membrane separation properties in terms of both flux and selectivity. Therefore, the reaction activities of amine groups (or membrane affinity) should be regarded in a broad sense, comprising not only the favorable and rapid reaction/interaction with CO_2 molecules but also the promoted/inhibited motion of CO_2 within amine-containing membranes. Consequently, to push the CO_2 separation performance (or transport efficiency) of these membranes to the limit, the first idea to keep in mind in the design process should be to choose an amine-containing material with a convenient affinity for CO_2 molecules. In fact, the effects that amine type (primary, secondary, and tertiary), basicity (or *pKa*), and steric hindrance can exert on CO_2 sorption performance in terms of absorption/adsorption capacity and rate, as well as energy cost during the CO_2 regeneration/release process, have been extensively studied in the field of amine-based CO_2 sorbents (solid adsorbents or aqueous alkylamine solutions) [14–17]. It is common knowledge that tertiary and/or sterically hindered amines in some cases could exceed the trade-off between the heat of reaction and the CO_2 absorption rate (see Figure 1), which thus enables energy-saving CO_2 sorption and release processes. Theoretically, this phenomenon could offer innovations for the design and development of amine-containing CO_2 separation membranes that integrate CO_2 adsorption, diffusion, and desorption processes into a thin membrane layer. Indeed, Prof. Ho's group developed and studied a series of CO_2-selective polymeric membranes containing sterically hindered polyamines [18–20]. They found that the steric hindrance effect of polyamines could significantly promote CO_2 transport performance in both CO_2 permeability and CO_2/gas (gas = H_2, N_2) selectivity, and this trend was more distinct in the case of moderately hindered polyamines (see Figure 2) [18]. Unfortunately, only a very limited number of systematic studies providing simultaneous CO_2 adsorption and diffusion/desorption kinetic properties have been devoted to amine-functionalized, silica-based membranes. Given this, in our earlier studies, we developed a series of amine-containing organosilica membranes including unhindered (PA-Si, SA-Si) and sterically hindered (TA-Si, BTPP) amines, as well as a quaternary ammonium salt (QA-Si), and investigated the effect that amine type exerted on the CO_2 adsorption/desorption properties of solid powders and the related membrane performance (see Figure 3) [21–24]. It seems really important to more systematically compare the CO_2 separation performance of amine-functionalized silica-based membranes, despite many review papers for CO_2 separation membranes in the literature, which mostly review hydrocarbon-based membranes [4,25]. In this review, we briefly summarize studies on amine-functionalized silica/organosilica membranes and pay special attention to the role of amine type in CO_2 separation performance. Synthesis approaches, characterizations of the xerogel powders in terms of CO_2 adsorption/desorption properties, and comparison of CO_2 transport behaviors within related membranes are included. Furthermore, future prospects and possible directions for the design and fabrication of amine-containing membranes for CO_2 separation are also presented, and this portion is not limited to silica-based membranes.

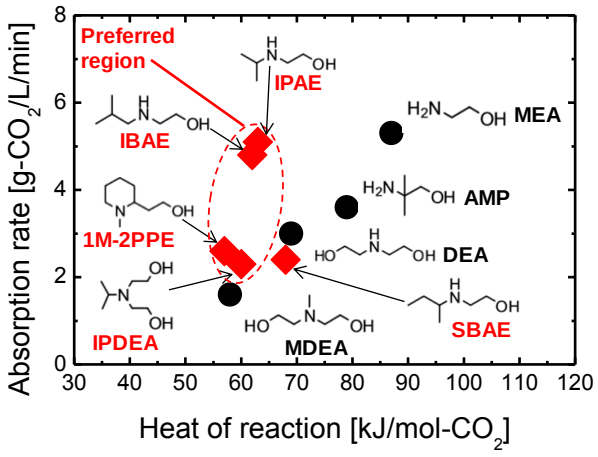

Figure 1. Relationships of absorption rate and heat of reaction between conventional and synthesized amines employed for CO_2 absorbents. Solid circles (●): conventional amines with no/low steric hindrance. Solid diamond (◆): synthesized amines with sterical hindrance. Abbreviations: **MEA**, 2-aminoethanol; **AMP**, 2-amino-2-methyl-1-propanol; **DEA**, diethanolamine; **MDEA**, methyldiethanolamine; **IPAE**, 2-(isopropylamino)ethanol; **IBAE**, 2-(isobutylamino)ethanol; **SBAE**, 2-(secondarybutyamino)ethanol; **IPDEA**, 2-(isopropyl)diethanolamine; **1M-2PPE**, 1-Methyl-2-piperidineethanol. Generally, there is a trade-off relationship between the heat of reaction and the absorption rate for conventional amines. However, the introduction of steric hindrance creates a unique performance that features a low heat of reaction but results in a moderately high absorption rate. The data were adapted from ref. [15].

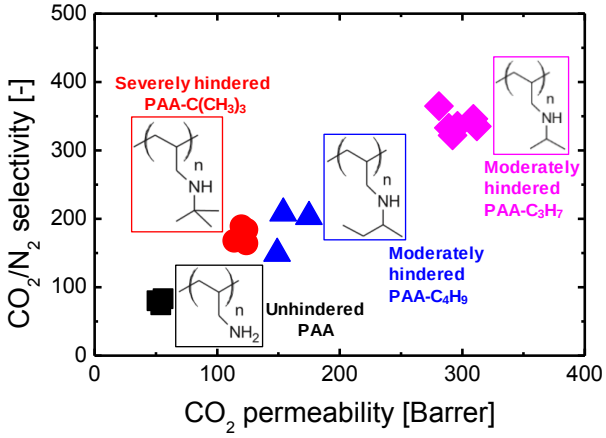

Figure 2. CO_2 separation performance comparison regarding the steric hindrance effect of polyamines for polyallylamine (PAA) membranes. CO_2/N_2 separation was performed at 110 ℃ and a feed pressure of 2 bar with water injection rates = 0.03/0.03 cm^3/min (feed/sweep) using a feed gas composition of 20% CO_2, 40% H_2, and 40% N_2 (on dry basis). The data was adapted from ref. [18].

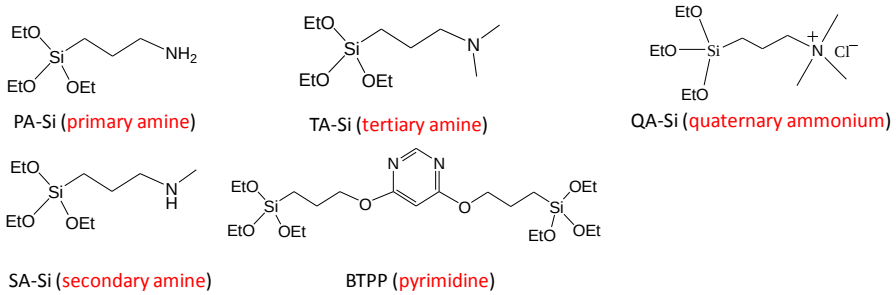

Figure 3. Chemical structures of amine-containing organosilica precursors employed in Prof. Tsuru's group.

2. Classifications and Reaction Activities between CO_2 and Amines

Amines are typically sub-classified as primary, secondary, or tertiary based on the degree of hydrocarbon substitution, while they also can be sub-classified as aliphatic, cycloaliphatic, aromatic, or heterocyclic. The diverse structures of amines confer basicity and a reaction activity that varies with acidic molecules (e.g., CO_2, H_2S). Generally, there are three factors that influence amine basicity: alkyl group substitution (including solvation effects and steric hindrance), resonance effect, and hybridization effect. The interlaced influences complicate the actual situation and make it more difficult to predict the down-to-earth basicity (or even the basicity order), which, however, can be reflected by the actual measurement of *pKa*. Consequently, the normal aliphatic amines of primary, secondary and tertiary types are all of approximately equal basicity, which is generally stronger than aromatic amines. Notwithstanding, it is the steric hindrance effect rather than amine basicity that plays a key role in impacting their reaction activities with CO_2. Usually, a normal aliphatic primary or secondary amine can form a zwitterion upon encountering a CO_2 molecule (Equation (1)) and can then proceed with the formation of a fairly stable carbamate complex with another amine group (Equation (2)). Under humid conditions, this carbamate complex can further react with a water molecule and form a bicarbonate ion and a free amine group (Equation (3)) [26].

$$RR^*NH + CO_2 \leftrightarrow RR^*NH^+COO^- \quad (1)$$

$$RR^*NH^+COO^- + RR^*NH \leftrightarrow RR^*NCOO^- + RR^*NH_2^+ \quad (2)$$

$$RR^*NCOO^- + H_2O \leftrightarrow RR^*NH + HCO_3^- \quad (3)$$

In Equations (1) to (3), R^* represents a H atom for a primary amine or another alkyl group. Equation (1) is a nucleophilic addition reaction, which is the rate-limiting process regardless of whether water is involved. Equations (2) and (3), however, represent rapid proton transfer reactions [27]. Tertiary amines, sterically hindered or not, on the other hand, owing to the lack of free hydrogen atom, are unable to react directly with CO_2 to form a carbamate. Instead, an alternative reaction occurs preferably to form a bicarbonate ion under humid conditions (Equation (4)) [28].

$$RR^*R^{**}N + CO_2 + H_2O \leftrightarrow RR^*R^{**}NH^+ + HCO_3^- \quad (4)$$

where R, R^* and R^{**} could be either different or identical alkyl groups.

Sterically hindered amines (SHAs), as originally defined by Sartori and Savage, can be identified from either of the following: (i) a primary amine in which the amino group is attached to a tertiary carbon atom or (ii) a secondary amine in which the amino group is attached to at least one secondary or tertiary carbon atom [29]. Based on this definition, it is difficult to identify tertiary amines with small bulkiness. In this review, we regard tertiary amines as SHAs due to their similar performance. Unlike unhindered amines, SHAs are characterized by the formation of carbamates with intermediate-to-low stability due to the bulkiness of the substitutions attached to the amino groups. In this way, SHAs may provide a faster reaction with CO_2 while they lower the heat of reaction. As such, membranes with SHAs might proceed with CO_2 transport (adsorption-hop-desorption) more effectively across the membrane thickness. In addition, as shown in Equations (3) and (4), humidity or water vapor is also an important factor that impacts the CO_2 transport behaviors within amine-containing membranes, which might make it more complicated to investigate the role of amine type in CO_2 transport behaviors. The effect of humidity on CO_2 transport behaviors was therefore excluded in this review.

3. Synthesis of Amine-Functionalized Silica/Organosilica Membranes

In general, amine-functionalized silica-based membranes are mainly fabricated via either (i) direct sol-gel processing from amine-functionalized silica precursors [6,7,30] or (ii) post-grafting or impregnation of mesoporous silica membranes [11–13]. In addition, the chemical vapor deposition (CVD) method is also sometimes used for the direct deposition of amine-functionalized silica precursor on the substrates, which suggests advantages to prepare defect-free membranes compared with the sol-gel route [10]. However, this method consists of a thermal decomposition step for the

silica precursor at higher temperatures (generally > 400°C) prior to the deposition process, which could result in the degradation of most amine groups.

3.1. Sol-Gel Route

The sol-gel technique is commonly used in the preparation of silica-based membranes, and it allows the hydrolysis and condensation processes to be performed under mild conditions (low-to-moderate temperature). Therefore, amine-functionalized silica-based membranes fabricated via sol-gel processing retain as much of amine groups as possible. To achieve uniform architectures with intercrystallite voids ranging from nano or sub-nano levels, the so-called "polymer" route is always considered. As mentioned above, in our earlier work, by adopting this method, as well as a moderate calcination temperature, we developed a series of amine-containing organosilica membranes for the utmost retention of amine groups. Following a similar route, much effort has been devoted to the fabrication of amine-functionalized silica-based membranes with microporous or nonporous microstructures [6,7,30]. The synthesis conditions and membrane performance are briefly summarized in Table 1. Note that these reported membranes have demonstrated scattered results concerning CO_2 separation performance in terms of permeance and selectivity. To some extent, the possible defects usually presented in silica-based membranes combined with a relatively wider pore size distribution may result in poor CO_2 separation performance. On the other hand, unhindered amines, such as APTES, were generally employed to serve as active sites for the reversible reactions with CO_2, which might show confined CO_2 mobility within these membranes due to the formation of stable carbamates. In cases, such as refs. [6,30], membranes with precisely controlled pore sizes have demonstrated relatively high CO_2 separation performance. However, in those studies, the effect that amine type exerted on the membrane performance was not involved. In our previous studies, membranes with tertiary or sterically hindered amines showed a greater potential for CO_2 separation compared with membranes that contain unhindered amines fabricated under the same conditions. These studies are systematically compared here.

Table 1. Summary of synthesis conditions and membrane performance for reported amine-functionalized silica-based membranes fabricated via a sol-gel route.

Precursors Used	Calcination Temperature [°C] [a]	Operation Temperature [°C] [b]	CO_2 Permeance [10^{-10} mol/(m^2 s Pa)]	CO_2/N_2 Selectivity [-]	Ref.
TEOS, APTES,	300-350 (vacuum)	22	100–800	40–80 [c]	[6]
TEOS, GlyNa	300–350 (vacuum)	22	100–400	50–100 [c]	[6]
TEOS, APTES	300–500	22	70	55 [c]	[30]
BTESE, APTES	250	50	~350	1–10 [d]	[7]
APTES	300	35	30	8 [d]	[21]
BTPP	300	35	337	25 [d]	[21]
PA-Si	250	35	260	22 [d]	[22]
SA-Si	250	35	170	11 [d]	[22]
TA-Si	250	35	1720	21 [d]	[22]
QA-180 [e]	180	35	40	4 [d]	[23]
QA-180-250	250	35	520	24 [d]	[23]
QA-250	250	35	490	18 [d]	[23]

[a] The temperature used for the membrane formation. [b] The temperature operated for gas permeation test. [c] Separation factor of a mixed system. [d] Ideal selectivity. [e] QA-180 represents a quaternary ammonium-silica membrane fired at 180 °C. Abbreviations: **TEOS**, tetraethoxysilane; **APTES** and **PA-Si**, 3-aminopropyltriethoxysilane; **GlyNa**, sodium glycinate; **BTESE**, 1,2-Bis(triethoxysilyl)ethane; **BTPP**, 4,6-bis(3-triethoxysilyl-1-propoxy)-1,3-pyrimidine; **SA-Si**, 3-(triethoxysilyl)-*N*-methylpropan-1-amine, **TA-Si**, 3-(triethoxysilyl)-*N*,*N*-dimethylpropan-1-amine, **QA-180**, Trimethyl[3-(trimethoxysilyl)propy]ammonium chloride derived membrane fired at 180 °C; **QA-180-250**, Trimethyl[3-(trimethoxysilyl)propy]ammonium chloride derived membrane fired at 180 °C before a post-heat-treatment at 250 °C; **QA-250**, Trimethyl[3-(trimethoxysilyl)propy]ammonium chloride derived membrane fired at 250 °C.

3.2. Post-Treatment of Mesoporous Silica Membranes

Mesoporous silica membranes with pore sizes ranging from 2–50 nm are ineffective for CO_2 separation. The meso-pores of these membranes could be minished, however, by the post-grafting or impregnation of amine-containing agents to impart high separation performance. Post-impregnation methods involve the loading of a large quantity of amines dissolved in a solvent inside the meso-pores. However, the loaded amines tend to conglomerate, and/or leak out from the pores, particularly under pressurized gas flow [31]. On the other hand, during the post-grafting process, the amine groups from the functionalized agents could be covalently attached to the pore/membrane surface, and a certain proportion of Si atoms could be replaced by aminosilane groups. This approach roughly maintains the structure of the substrate, and the grafted amine groups remain stable [31]. Numerous studies have described amine-functionalized silica-based membranes [11–13,32,33]. Table 2 lists the synthesis conditions and membrane performance for reported amine-functionalized silica-based membranes fabricated via post-grafting or impregnation. Similar to those produced via sol-gel routes, reports of these membranes show CO_2 separation properties that are even more scattered with either low permeance or low CO_2/N_2 selectivity. This phenomenon probably can be attributed to the relatively larger pore size of the mesoporous support as well as to the excessively strong affinity to CO_2 of these unhindered amines (APTES etc.), which can limit the CO_2 transport rate. With the respect to formation of dense membranes via post-grafting, these membranes tended to show relatively high CO_2/N_2 selectivity due to the higher resistance to N_2 permeation. On the contrary, this formation of loose membranes may result in higher CO_2 permeance but lower CO_2/N_2 selectivity. Note that for practical process designs of membrane separation applications from an economic perspective, increases in membrane permeance are more important than increases in selectivity in order to enhance competitiveness for CO_2 capture of flue gas [34]. In addition, amine-containing facilitated membranes are expected to simultaneously promote both CO_2 permeance and CO_2/gas selectivity via reversible reactions/interactions. However, this is not always true in the case of amine-functionalized silica-based membranes. Given that the membrane performance can be generally governed by parameters such as the materials used for the selective layer, the geometry and performance of the support, and the preparation technique adopted, systematic studies are needed to address unexpected and somewhat disappointing performances.

Table 2. Summary of synthesis conditions and membrane performance for reported amine-functionalized silica-based membranes fabricated via post-treatment of mesoporous silica-based membranes.

Membrane Support	Functionalized Agent	Temperature [°C] [a]	CO_2 Permeance [10^{-10} mol/(m^2 s Pa)]	CO_2/N_2 Selectivity [-]	Ref.
Vycor tubes	APTES	120	1.8	10 [b]	[11]
Silica	APTES	100	10	800 [b]	[11]
Silica	Aziridine	35	~6	0.15 [c]	[13]
Silica	Aziridine	35	~10 (wet)	~3 [c]	[13]
Silica	TRIES, NH_3	200	2000	2 [c]	[32]
Silica	APTES	40	0.15	50 [b]	[33]
		40	0.023 (wet)	9 [b]	
		60	6.1	72 [b]	
		80	5.2	289 [b]	
		100	6.1	339 [b]	
Silica	TA	60	6.9	300 [b]	[33]
		60	0.11 (wet)	256 [b]	

[a] The temperature used for gas permeation testing. [b] Separation factor of a mixed system. [c] Ideal selectivity. Abbreviations: **APTES**, 3-aminopropyltriethoxysilane; **TRIES**, triethoxysilane; **TA**, 3-trimethoxysilylpropyl-diethylenetriamine.

4. Role of Amine Type in CO_2 Separation Performance

As mentioned above, this review pays special attention to surveys of the role of amine type in CO_2 transport behaviors through amine-functionalized silica-based membranes. Generally, CO_2 transport through a membrane involves adsorption in the membrane surface or pore walls, diffusion across the membrane thickness, and desorption from the membrane permeate side (see Figure 4a). All the processes to some extent can be affected by the materials' chemistry, while the diffusion process can be generally governed by both the materials' chemistry and the membrane microstructure (e.g., pore size, pore length, and porosity) (see Figure 4b). Therefore, to systematically investigate the role of amine type in CO_2 separation performance through a membrane, both materials' chemistry in terms of CO_2 adsorption/desorption properties and membrane microstructure should be involved simultaneously.

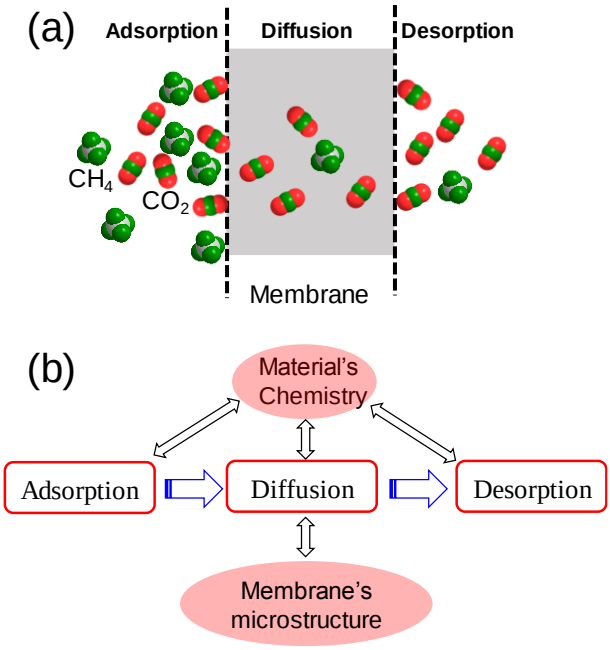

Figure 4. Schemes of (**a**) CO_2 separation through a membrane and (**b**) the factors impacting CO_2 transport behaviors including adsorption on the membrane surface, diffusion across the membrane thickness, and desorption from the membrane permeate surface.

4.1. Thermal Stability and Texture Microstructure

Generally, amorphous silica-based membranes should be fabricated at a calcination temperature that is sufficiently high to provide a well-crosslinked silica-based network for precise separation. Consequently, to prepare amine-functionalized silica-based membranes via a sol-gel route a moderate calcination temperature should be considered to avoid the thermal degradation of amine groups. Typically, there are two types of alkylamine degradation: thermal and oxidative [35]. Hence, to retain the utmost level of amine groups in the amine-functionalized membranes, both a sufficiently "safe" calcination temperature and an inert calcination atmosphere (e.g., He, N_2) must be considered. The thermal stability of alkylamine groups contained in silica-based matrix usually can be determined via methods such as Fourier transform infrared (FTIR) spectroscopy, energy dispersive spectroscopy (EDS), and X-Ray photoelectron spectroscopy (XPS) analysis, while the amine density, if necessary, can be quantitatively assessed via XPS analysis. To rationally investigate the role of amine type on CO_2 transport behaviors, first, the availability and density of the amine types should be at comparable levels, since this plays a considerable role in CO_2 transport behavior. In our earlier studies [22] comparing CO_2 separation performance among three amine-functionalized organosilica membranes (PA-Si, SA-Si, and TA-Si, see Figure 3 for their chemical structures), we evaluated the amine state and density for these amine-containing solid powders, as shown in Figure 5 and Table 3.

Generally, both free amine groups (C-NH_x, x = 0–2) and protonated amine groups (C-N^+H_x, x = 1–3) induced by surface Si-OH groups or a small amount of adsorbed CO_2 molecules could be observed for samples using different amine types (see Figure 5). In addition, all samples demonstrated comparable levels in amine density that were also comparable to their expected values as shown in Table 3. This indicated that the amine groups survived under the adopted calcination conditions (at 250 °C under a N_2 atmosphere) which enabled investigation of the effects amine type on membrane performance. In addition, it is worth to note that in the practical applications the activity and stability of amine groups can also be evidently affected by the presence of toxic components such as H_2S and water steam. These factors, unfortunately, have not always been involved in investigations of the operation stabilities for amine-containing membranes, and, therefore, relevant systematic studies are anticipated.

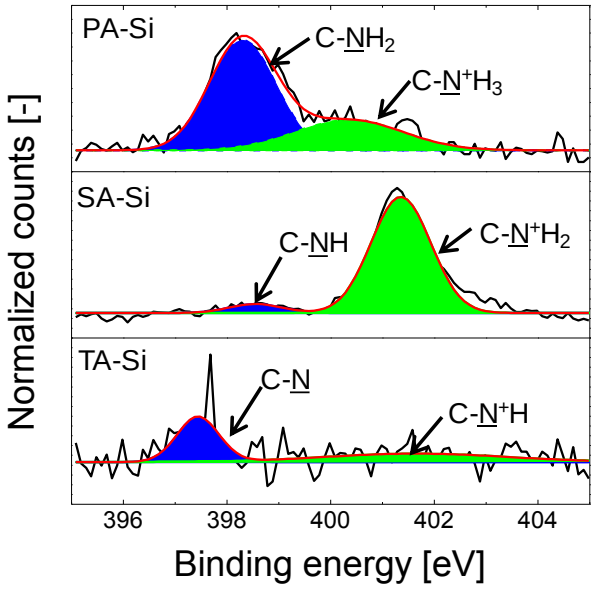

Figure 5. The N1s spectra of amine-silica xerogel powders fired at 250 °C under N_2 (black line, original peak; red line, fitted peak). Reproduced from ref. [22] with permission. Copyright (2017), *Elsevier*.

Table 3. Atomic composition of amine-silica xerogel powders fired at 250 °C estimated by XPS measurement. Reproduced from ref. [22] with permission. Copyright (2017), *Elsevier*.

Sample	Atomic Composition [%]				Amine (N) Density [mmol/g]	
	C1s	O1s	N1s	Si2s	Detected	Expected [a]
PA-Si	63.4	16.3	9.6	10.7	7.4	9.1
SA-Si	67.9	15.8	7.3	9.0	6.4	8.1
TA-Si	75.2	11.0	6.1	7.0	6.7	7.2

[a] The expected values of amine density data were calculated based on the general structural formula of $SiO_{1.5}R$ (R = alkylamine) of amine-silica xerogels, which assumes complete hydrolysis and condensation.

The physical microstructure of these amine-functionalized silica-based materials is also a very important factor, because this decides CO_2 transport behavior. Gas (N_2, CO_2 etc.) adsorption measurement is a typical approach for the determination of the texture microstructure of micro-to-mesoporous materials, which includes silica-based materials. Following the incorporation of alkylamine moieties, however, a possible dual flexible-rigid network can be formed, and therefore an apparently nonporous structure was observed, as evidenced by the N_2 adsorption/desorption isotherms operated at 77 K. This phenomenon was also generally observed in the cases of organic-rich organosilica membranes, as reported elsewhere [21,24,36]. Figure 6 shows the N_2 adsorption/desorption isotherms of several amine-functionalized organosilica materials in our earlier

studies. The negligible N_2 adsorption amount (<0.2 cm^3[STP]/g) for all the powders indicates the formation of a dual flexible-rigid network, in which "free-volume pores" were created instead of rigid pores. Therefore, without special interactions the adsorption of N_2 on the rigid surfaces/pores or voids was significantly prohibited, particularly at an extremely low temperature (e.g., 77 K) that could freeze the flexible organic chains. CO_2, however, could dissolve into the flexible organic phase and react with amine groups at a mild temperature (e.g., 35 °C) to be discussed hereinafter. Note that amorphous silica/organosilica materials/membranes fabricated via sol-gel routes generally demonstrate ultramicropores (<0.7 nm), whereas N_2 adsorption/desorption methods fail to characterize these very narrow pores. Alternatively, positron annihilation lifetime spectroscopy (PALS) measurement sometimes can be adopted to assess these dual flexible-rigid microstructures in terms of pore radius (rigid pores or free-volume pores) and fractional free volume (FFV) [23]. Figure 7 shows a typical example of PALS measurement on quaternary ammonium-silica films fired at different temperatures. Although N_2 adsorption measurement reveals no differences between those two films, PALS measurement can obviously detect the differences between them due to the differences in calcination temperatures that result in a local liberation of small molecules (CH_3Cl) and in the subsequent formation of ultra-micropores [23]. The pore sizes of these materials in the ultra-micro level (0.2–0.7 nm) have been discussed in detail elsewhere [23].

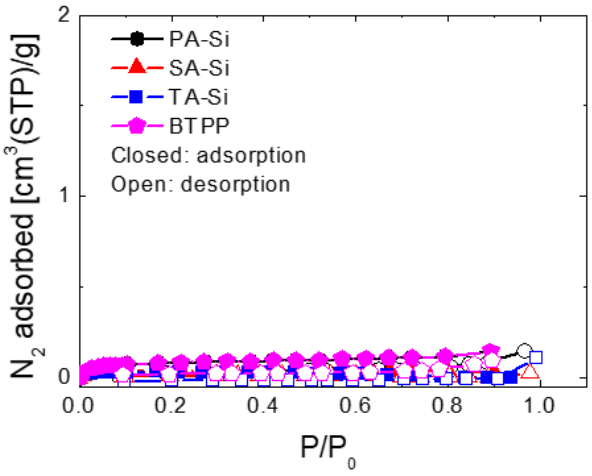

Figure 6. N_2 adsorption/desorption isotherms of several amine-functionalized organosilica materials fired at a "safe" temperature (300 °C for BTPP and 250 °C for PA-Si, SA-Si, and TA-Si) under a N_2 atmosphere. These results were reorganized from refs. [21,22].

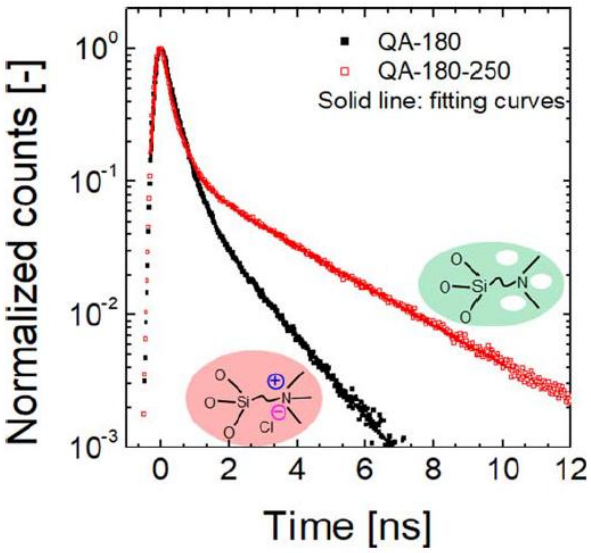

Figure 7. PALS data for quaternary ammonium-silica films fabricated on silica wafers, as recorded at a positron incident energy level of 1.2 keV. QA-180: Trimethyl[3-(trimethoxysilyl)propy]ammonium chloride-derived film fired at 180 °C; QA-180-250: Trimethyl[3-(trimethoxysilyl)propy]ammonium chloride-derived film fired at 180 °C before post-heat-treatment at 250 °C. Both samples were fired under a N_2 atmosphere, so was the post-heat-treatment. Reproduced from ref. [23] with permission. Copyright (2017), John Wiley and Sons.

4.2. Reaction Activities of Amines

Acid catalysts (HCl, etc.) are generally required during the preparation of *polymer* sols to perform hydrolysis for membrane preparation via a sol-gel route. In addition, sometimes, an excessive amount of acid should be used in some cases to avoid the gelation of sols due to the basic nature of amine groups. Thus, after the membrane formation, the reactivation of these temporarily deactivated amine groups should be taken into consideration. Generally, either calcination at sufficiently high temperatures or vacuum calcination has been adopted to remove acidic molecules used for sol preparation. However, different alkylamines vary in reaction activities with acidic molecules, which may depend on the degree of basicity as well as on steric hindrance. Figure 8 shows the temperature dependence of HCl removal for two different amine-functionalized organosilica materials in one of our earlier studies [21]. APTES, with unhindered primary amine groups, demonstrated greater difficulties for the removal of the stable HCl that existed at temperatures as high as 200 °C. By contrast, in the case of BTPP with pyrimidine (hindered amine) groups, HCl had started to diminish at the first measured temperature, which was as low as 50 °C. Hence, a temperature of higher than 200 °C should be used to reactivate the amine groups, particularly for unhindered amines. Note that calcination under vacuum could to some extent lower the temperature employed. On the other hand, this result indicated that unhindered amines and sterically hindered amines showed very different reaction/interaction activities with acidic molecules. Furthermore, the different reaction activities may play an important role in CO_2 transport behaviors across the relevant membranes. In another study [34], we also investigated the HCl removal among three amine-functionalized organosilica materials (PA-Si, SA-Si, and TA-Si shown in Figure 3) via EDS measurement. Figure 9 shows the HCl removal of these xerogel powders as a function of post-heat-treatment. After post-heat-treatment at 250 °C, the Cl signals almost disappeared for all three samples, but the removal rate was variable due to the differences in reaction activities with HCl (see Table 4). Specifically, HCl can be much easier to remove from xerogel powders in the case of TA-Si with tertiary amines compared with the other two samples with primary (PA-Si) or secondary (SA-Si) amines.

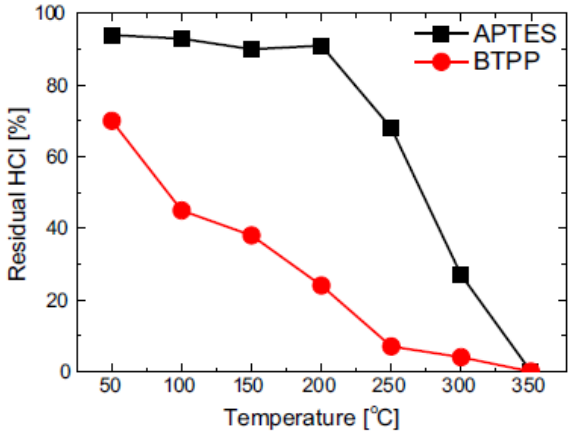

Figure 8. Temperature dependence of residual HCl in APTES and BTPP xerogel powders measured via EDS. The mole ratios of HCl/NH_2 = 1 for APTES and HCl/pyridine = 1 for BTPP were employed in the preparation of *polymer* sols. Prior to EDS measurement, APTES and BTPP xerogel powders prepared by drying the solvent of the sols at ~50 °C, were fired under N_2 for 30 min at 50, 100, 150, 200, 250, 300, and 250 °C. The molar compositions of the elements of Cl and Si were recorded and then the ratios of Cl/NH_2 for APTES and Cl/pyrimidine for BTPP were calculated by assuming molar ratios

of Si over either NH_2 or pyrimidine groups that were the same as those of the associated precursors. Reproduced from ref. [21] with permission. Copyright (2017), Elsevier.

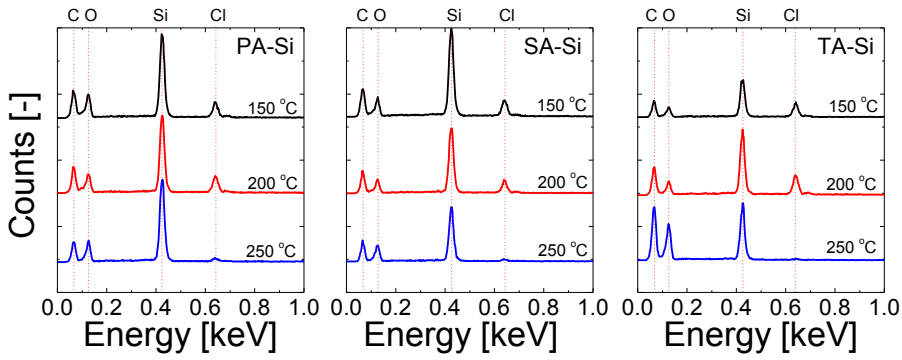

Figure 9. EDS profiles of amine-silica xerogel powders as a function of post-heat-treatment temperature (N_2 atmosphere, 30 min). Reproduced from ref. [22] with permission. Copyright (2017), *Elsevier*.

Table 4. Residual Cl content in amine-silica xerogel powders as a function of post-heat-treatment temperature (N_2 atmosphere, 30 min). Reproduced from ref. [22] with permission. Copyright (2017), *Elsevier*.

Material		Post-Heat-Treatment Temperature [°C]		
		150	**200**	**250**
PA-Si	Cl (at. %)	3.37	3.50	0.79
	Cl/Si (molar ratio) [a]	0.26	0.28	0.048
SA-Si	Cl (at. %)	3.31	3.34	0.63
	Cl/Si (molar ratio)	0.25	0.26	0.046
TA-Si	Cl (at. %)	4.8	4.3	0.14
	Cl/Si (molar ratio)	0.49	0.42	0.017

[a] The original Cl/Si molar ratio for the relevant PA-Si sol was 0.3, so were the ratios of SA-Si and TA-Si.

4.3. CO_2 Adsorption/Desorption Behaviors

As mentioned above, CO_2 adsorption/desorption behaviors are important factors that probably largely affect their transport behaviors across amine-containing membranes. Therefore, this review summarizes CO_2 adsorption/desorption properties including both static (measured by adsorption isotherms) and kinetic (measured by TG/DTA method) evaluations for the amine-functionalized organosilica materials studied in our previous studies [13,34]. Figure 10 shows the CO_2 adsorption/desorption isotherms at 35 °C for four amine-functionalized organosilica xerogel powders with unhindered amines (left figure), as well as for tertiary and sterically hindered amines (right figure). It should be apparent that the xerogel powders with unhindered amines demonstrated irreversible Langmuir-dominant adsorption/desorption isotherms with hysteresis loops probably due to the formation of stable carbamates after CO_2 adsorption, whereas tertiary and sterically hindered amines showed almost reversible Henry-dominant adsorption/desorption isotherms. Generally, CO_2 adsorption behaviors on amine-functionalized solid materials can be described by a dual-mode sorption model as a combination of Langmuir-type and Henry-type sorption as discussed in our earlier studies [23]. Note that SA-Si displayed a much higher adsorption capacity than the other three samples, which were comparable, presumably due to a somewhat stronger basicity that could improve the reaction capacity [10,37,38]. In addition to adsorption/desorption isotherms, the values of the isosteric adsorption heat of CO_2 (Q_{st}), which can also be regarded as CO_2 binding energy, for these xerogel powders were also calculated using *Clausius-Clapeyron* equation, as summarized in Figure 11. Consistent with their adsorption type, xerogel powders with unhindered amines presented

impressively higher levels of adsorption heat at lower levels of CO_2 uptake by comparison with hindered amines. However, their adsorption heat decreased rapidly as the CO_2 uptake increased before reaching a 30% level of CO_2 saturated sorption, which suggested the presence of heterogeneous surfaces containing alkylamine moieties and Si-O-Si (or Si-OH) networks. On the contrary, xerogel powders with hindered amines demonstrated intermediate-to-low values for Q_{st} throughout the adsorption process. Generally, Q_{st} also can be regarded as CO_2 binding energy, and higher values equate to greater difficulties for CO_2 desorption. It is interesting that the kinetic CO_2 adsorption/desorption results measured by TG/DTA methods verified the different difficulties among these xerogel powders, as shown in Figure 12. It seems that all samples demonstrated a fairly fast adsorption process regardless of amine type but demonstrated significant differences in the CO_2 desorption processes. The xerogel powders with unhindered amines displayed impressively higher irreversible adsorption capacities, particularly in the case of PA-Si. On the contrary, xerogel powders with hindered amines showed a lower, or at least a negligible, irreversible adsorption capacity with a much faster desorption rate.

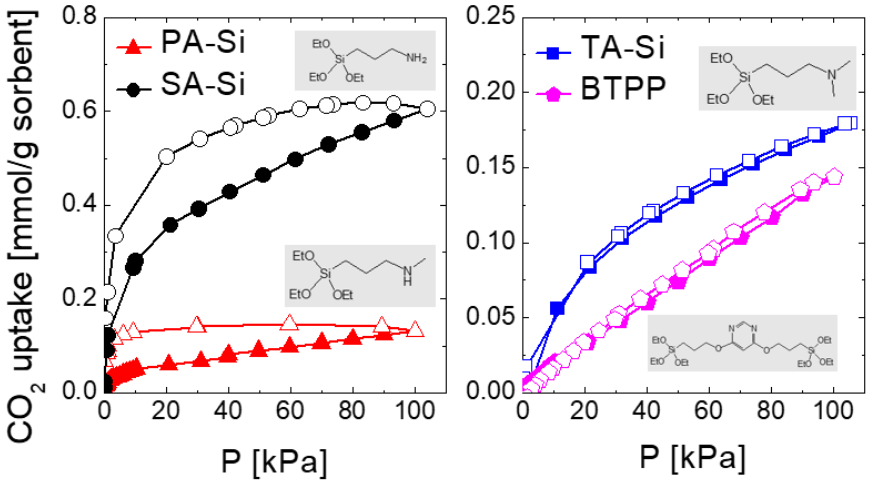

Figure 10. CO_2 adsorption/desorption isotherms at 35 °C for amine-functionalized organosilica xerogel powders. The solid symbols represent the adsorption data, and the open symbols show desorption. Results were reorganized from refs. [21,22].

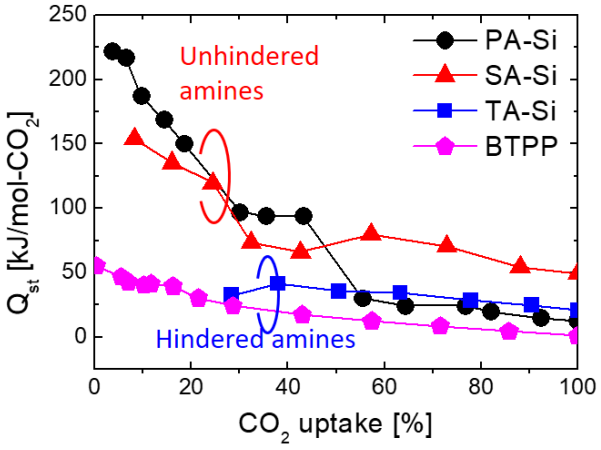

Figure 11. Isosteric adsorption heat of CO_2 for amine-functionalized organosilica xerogel powders calculated from adsorption isotherms. Adsorption isotherms measured at 35, 45 and 55 °C were adopted for the calculation and the values of CO_2 uptake were normalized using each maximum adsorption capacity (at 100 kPa) as a standard. Results were reorganized form refs. [21,22].

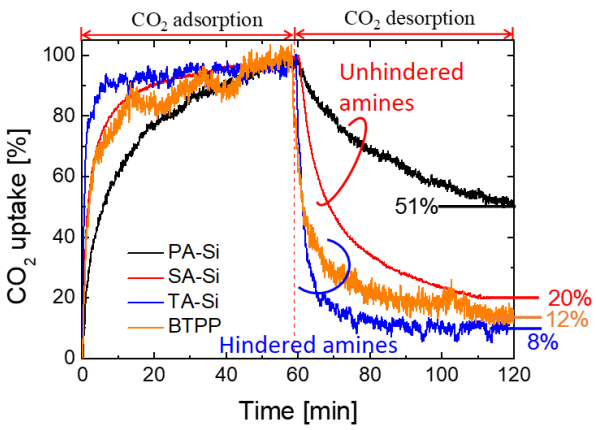

Figure 12. Time course of normalized CO_2 adsorption amount for the 1st cycle of a CO_2 adsorption/desorption process for amine-functionalized organosilica xerogel powders performed on TG/DTA equipment. A 60 vol% of CO_2 in a CO_2-Ar mixture with a flow rate of 50 cm^3/min and a total pressure of 100 kPa was adopted for the CO_2 adsorption process, while pure Ar with the same flow rate and pressure was used for CO_2 desorption process. The samples were activated by heating at 200 °C for 12 h, followed by cooling to 35 °C under a pure Ar atmosphere. Results were reorganized from refs. [21,22].

4.4. Gas Permeation Properties

As discussed above, the amine-functionalized organosilica xerogel powders developed in our previous studies showed comparable microstructures but different reaction activities with acidic molecules with impressively different CO_2 adsorption/desorption properties. Gas permeation performance for these relevant membranes was then collected to investigate of the roles of amine type in CO_2 transport behaviors.

Figure 13 shows the kinetic diameter dependence of gas permeance for amine-functionalized organosilica membranes. All the synthesized membranes demonstrated sufficiently high qualities with He/SF_6 selectivities of 3000–40,000. In addition, these membranes displayed comparable gas permeation performance (actual or normalized permeance) in terms of kinetic diameter dependence, probably due to their similar chemical structures or ratios of organic/silica. Note that both the sufficiently high qualities and comparable structures could to some extent enable investigation into the effect of amine type on CO_2 transport performance. Figure 14 compares the temperature dependence of gas permeance for amine-functionalized organosilica membranes. Generally, the temperature dependence of gas permeance values with a wide spectrum that was enabled by the superior thermal stability of organosilica membranes, could offer important information on gas-transport mechanisms. As shown in Figure 14, all the gases considered led to a linear relationship for gas permeance in the logarithmic coordinates vs. *1000/T*, which can be accurately represented by *Arrhenius*-type equations. Universally, gaseous transport through microporous or dense membranes requires sorption (adsorption onto the pore walls and/or dissolution into a nonporous phase) of gas molecules prior to the subsequent diffusion process and demonstrates several types of temperature dependence. Therefore, the gas permeance (P) that is a product of the diffusivity (D) and solubility (S) coefficients ($Pl = DS$, where l is the membrane thickness), as well as the diffusivity coefficient (D), could also be represented using *Arrhenius*-type equations. Meanwhile, the solubility coefficient (S) is usually described via *Van't Hoff* expression [39–42].

$$P = P_0 exp(\frac{-E_p}{RT}), \quad (5)$$

$$D = D_0 \exp(\frac{-E_d}{RT}), \quad (6)$$

$$S = S_0 \exp(\frac{-\Delta H_s}{RT}), \quad (7)$$

In Equations (5)–(7), P_0, D_0, and S_0 are the pre-exponential factors, E_p and E_d are the apparent activation energies for permeation and diffusion, respectively, ΔH_s is the effective sorption enthalpy, R is the universal gas constant, and T is the operation temperature. A relationship among E_p, E_d and ΔH_s can then be obtained after the combination of Equations (5)–(7) when $Pl = DS$, as shown in Equation (8).

$$E_p = E_d + \Delta H_s, \quad (8)$$

The gas permeance of all the gases, except that of CO_2, was decreased with a decrease in the permeation temperature, indicating an activated transport mechanism ($E_p > 0$). Generally, the diffusivity of a penetrant is mainly decided by the relative difference between its kinetic diameter and the membrane pore size and/or the segment mobility of the membrane matrix, which demonstrates the ever-increasing nature of the function of temperature ($E_d > 0$). Whereas solubility is greatly influenced by the condensability (critical temperature) of the penetrant and by the affinity/interactions that the membrane matrix has with the penetrant, there often is also a decrease in the function of temperature ($\Delta H_s < 0$) [41,42]. Hence, He, H_2, N_2, and CH_4, which have no special interactions with amine groups, showed a significant level of activated diffusion ($E_p > 0$), suggesting that temperature has a greater effect on diffusivity than it does on solubility. However, for CO_2 that has strong interactions with amine groups as well as higher solubility in an organic-rich phase, the temperature dependence of permeance differed notably among these four amine-functionalized membranes. The details of these differences are hereinafter compared according to the activation energy for the permeation of CO_2 [$E_p(CO_2)$].

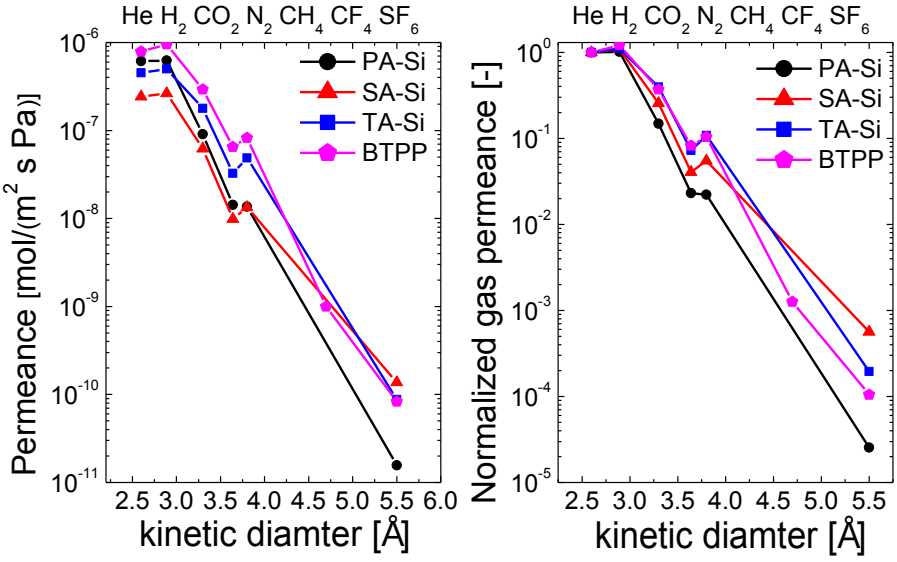

Figure 13. Kinetic diameter dependence of gas permeance (left: actual permeance; right: normalized permeance) operated at 200 °C for amine-functionalized organosilica membranes. The gas permeances were normalized based on their He permeances as standards. Results were reorganized from refs. [21,22].

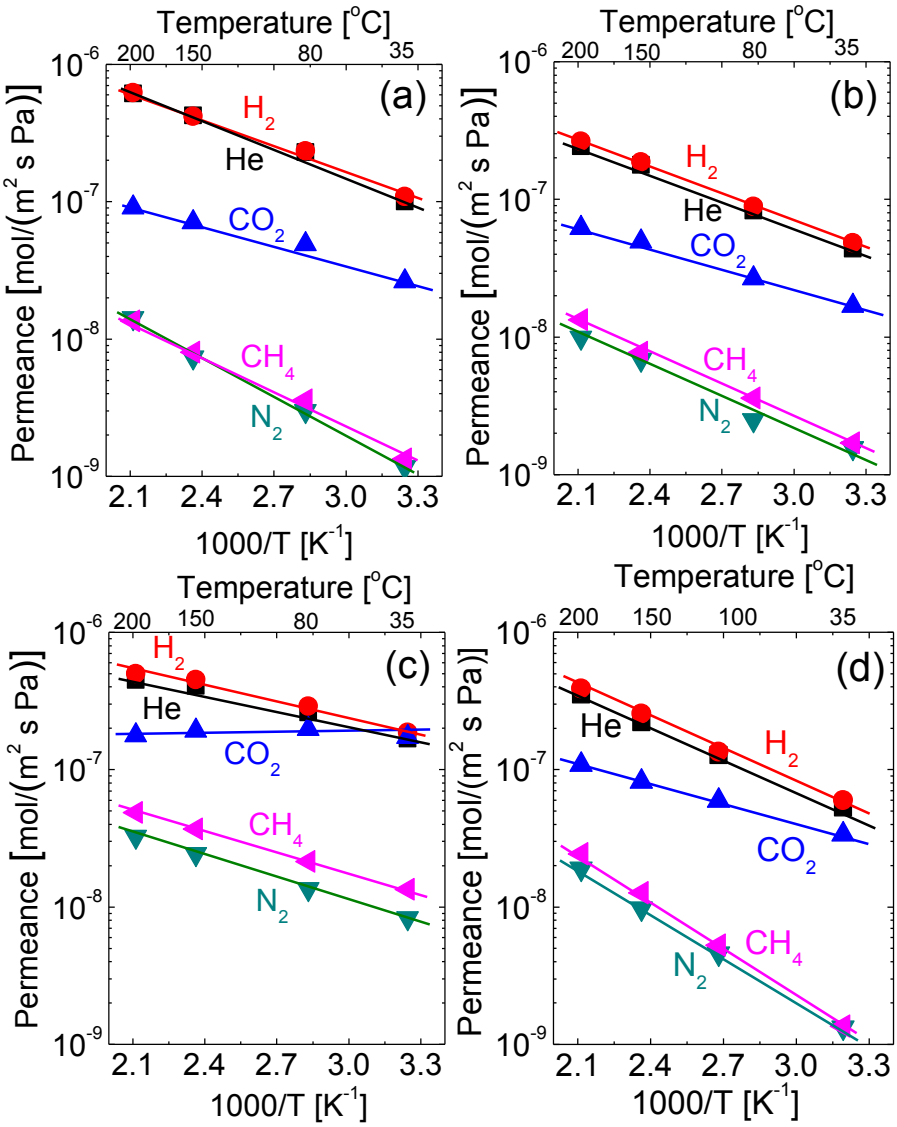

Figure 14. Temperature dependence of gas permeance for amine-functionalized organosilica membranes: (**a**) PA-Si, (**b**) SA-Si, (**c**) TA-Si, and (**d**) BTPP. Results were reorganized from refs. [21,22].

In addition to amine type, microporosity is another important factor impacting permeation performance of CO_2 as well as that of other gases. In one of our previous studies [23], we used a similar method to develop a microporosity-enhanced, amine-functionalized, organosilica membrane via the thermally induced local liberation effect of QA-Si. In that study, we observed a dealkylation reaction of quaternary ammonium groups at ~230 °C in polycondensed QA-Si derived membranes with the liberation of CH_3Cl molecules. The membranes after liberation of CH_3Cl via either direct calcination at 250 °C (QA-250) or post-heat treatment (QA-180-250) (see PALS data in Figure 7) demonstrated significantly improved gas permeation performance compared with the membrane fabricated from TA-Si without a liberation effect (see Figure 15). In the case of the liberation of CH_3Cl, a quaternary ammonium chloride was transformed to a tertiary amine group, in which the amine accessibility was improved as a result of the creation of microporosity around the tertiary amine groups.

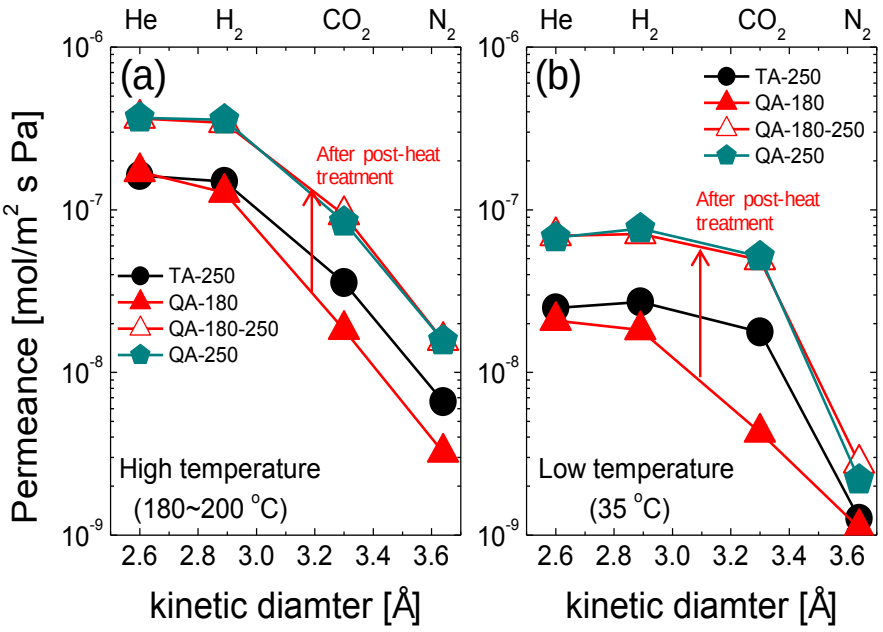

Figure 15. Kinetic diameter dependence of gas permeance for QA-Si derived membranes fired at different temperatures and performance comparison with TA-Si derived membranes at both (**a**) high and (**b**) low temperatures. Gas permeation test of QA-180 fabricated with a calcination temperature of 180 °C was performed at 180 °C and 200 °C for the remaining three membranes. Reproduced from ref. [23] with permission. Copyright (2017), John Wiley and Sons.

Figure 16 compares the trade-off between CO_2 permeance and CO_2/N_2 permselectivity of the amine-functionalized organosilica membranes developed by our group. The membranes functionalized with hindered amines tended to show superior CO_2 separation compared with those with unhindered amines as well as quaternary ammonium. In addition, the membranes with hindered amines demonstrated a greater ability to surpass the Robeson upper bound generally seen in polymeric membranes. Herein, the Robeson upper bound was plotted in the term of permeance rather than permeability by assuming a membrane thickness of 500 nm, due in large part to the difficulties in accurate determination of the thickness of very thin organosilica selective layer with interpenetrations into a nanoporous sublayer and due in part to the typical thickness of organosilica membranes that are estimated to range from 200 to 600 nm, as discussed elsewhere [23,24]. This implies that the hindered amines showed a greater advantage in facilitating CO_2 transport through amine-functionalized silica-based membranes (based on single gas permeation test), consistent with the results observed (based on binary gas separation test) by Prof. Ho's group (see Figure 2) [18–20]. Therefore, these results suggested that the amine type could play a coincidental role in CO_2 transport behaviors for either single or binary/mixed gas systems, given that the differences between single and mixed gas separation performance can be generally observed due to the competitive adsorption/interaction. This consistent tendency can probably be ascribed to the intermediate-to-low CO_2 binding energy of hindered amines that enables both fast adsorption on and fast diffusion/desorption through/from these membranes of CO_2 molecules, as illustrated in one of our previous studies (see Figure 17) [21]. Generally, all the gases could permeate across membranes via less-interactive diffusion while sorptive gases (CO_2, etc.) permeate the amine-functionalized membranes via interactive diffusion in addition to less-interactive diffusion. Different amine types could lead to different CO_2 binding energies and in turn to different sorption types. The CO_2 binding energy of the active carrier sites probably plays an important role in CO_2 transport efficiency considering the contribution of interactive diffusion. Owing to the formation of a stable carbamate or to strong CO_2-amine interactions with high CO_2 binding energy, a dual-mode sorption always occurs, and the effective CO_2 transport through membranes with unhindered amines (strong-affinity) may be restricted. On the other hand, by employing sterically hindered amines, reversible CO_2

adsorption/desorption behavior in the xerogel powders can be observed and a good balance between favorable adsorption and prohibited diffusion/desorption of CO_2 is thus expected in relevant membranes. As a result, more effective CO_2 transport through these membranes could be accomplished with an intermediate-to-low level of CO_2 binding energy. However, it is worth to note that in some cases enhanced affinity to CO_2 of a membrane was proposed to facilitate more favorable CO_2 sorption so as to limit access by other gases, resulting in a higher CO_2/gas selectivity in a mixed gas system [43]. Indeed, in a certain range, a higher CO_2 binding energy would improve CO_2/gas sorption selectivity and lead to a high separation performance. Nevertheless, this tendency generally occurs on the conditions that the increases in CO_2 binding energy (or adsorption heat) could not largely affect the reversible adsorption properties, since too sufficiently high CO_2 binding energy may result in irreversible CO_2 adsorption that cannot generate flux.

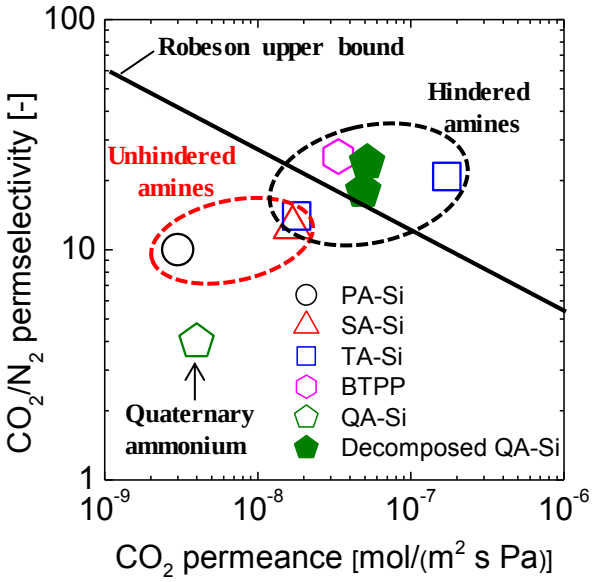

Figure 16. Comparison of CO_2 separation performance for amine-functionalized organosilica membranes at 35 °C. The Robeson upper bound was plotted by assuming a membrane thickness of 500 nm. Results were reorganized from refs. [21–23].

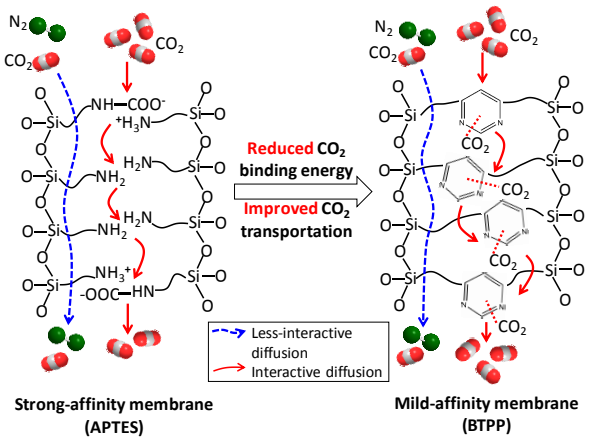

Figure 17. Comparison of CO_2 transport mechanisms across strong-affinity (APTES) and mild-affinity (BTPP) membranes. Reproduced from ref. [21] with permission. Copyright (2017), *Elsevier*.

4.5. Activation Energies for Gas Permeation

To further compare the influence of amine type on the CO_2 transport behaviors of these amine-functionalized organosilica membranes, the activation energies for the permeation (E_p) of CO_2 and N_2 in Equation (5) together with the relevant CO_2 separation performance are summarized in Table 4.

As mentioned above, E_p represents the sum of the activation energy for diffusion and the apparent adsorption enthalpy ($E_p = E_d + \Delta H_s > 0$), which reflects the total energy barriers for the permeation of gases. A higher E_p for a gas equates to a greater difficulty in permeation. Diffusivity depends on the kinetic diameter of the permeating gases and could be the rate-determining process for gas-permeation flux. On the other hand, CO_2 allowed strong interactions with the amine groups and exhibited significant sorption performance onto/into the rigid-pore surface and the organic nonporous phase, thereby allowing the effective solubility coefficient reflected by the negative value of sorption enthalpy (ΔH_s) to play a more critical role in the CO_2 permeation performance. The relatively higher negative value of $\Delta H_s(CO_2)$ led to a low total activation energy for permeation in the case of CO_2 [$E_p(CO_2)$]. Indeed, for all the membranes listed in Table 5. lower values for $E_p(CO_2)$ were always observed compared with that of $E_p(N_2)$, despite the comparable size between CO_2 (3.3 Å) and N_2 (3.64 Å).

In addition, the gas permselectivity, α_{ij}, could be quantitatively linked with the difference in the values for the activation energy of permeation, $E_{pi} - E_{pj}$, by considering $\alpha_{ij} = P_i/P_j$. As shown in Equation (9), α_{ij} could be expressed by an Arrhenius-type equation, similar to that of gas permeance and diffusivity.

$$\alpha_{ij} = \frac{P_{i0}}{P_{j0}} \exp\left(-\frac{E_{pi}-E_{pj}}{RT}\right) \propto \exp\left(-\frac{E_{pi}-E_{pj}}{RT}\right), \quad (9)$$

where P_{i0} and P_{j0} are pre-exponential factors for components i and j, respectively. Considering the possible differences in pre-exponential factors that may depend on the membrane and the penetrant, the negative values for the difference in E_p between a smaller/sorptive component, i, and a larger component, j ($E_{pi} - E_{pj}$), could to some extent reflect the potential in gas permselectivity for this gas pair (α_{ij}). Under a given system, higher negative values for $E_{pi} - E_{pj}$, would likely offer higher values for α_{ij}, and this trend might increase with a decrease in the operational temperature. As listed in Table 4, such a trend can be evident regardless of amine type.

Most importantly and specifically, the relationships between $E_p(CO_2)$ and $E_p(N_2)$, which could predict the CO_2/N_2 separation performance, are compared in Figure 18. Owing to a non-reactivity feature and to a kinetic size that approximates the membrane pore size, $E_p(N_2)$ has greater advantages to reflect the microstructure of these amine-functionalized organosilica membranes. Generally, higher values for $E_p(N_2)$ reflect the denser microstructure of silica-based membranes, and vice-versa. In a similar manner, the lower values for $E_p(CO_2)$ reflect the greater permeation potential for CO_2 when the relevant values of $E_p(N_2)$ are comparable. As Figure 18 shows, all the membranes with reproduced cases demonstrated comparable and scattered values of $E_p(N_2)$ at 10–20 kJ/mol, which indicated a similar microstructure regardless of amine type. However, membranes consisting of hindered amines presented an impressive trend of decreases in $E_p(CO_2)$ compared with membranes that have unhindered amines, which indicated that CO_2 was much more permeable across these membranes with hindered amines. In addition, with respect to membranes with unhindered amines (PA-Si and SA-Si), the PA-Si membranes tended to present a denser microstructure due to somewhat higher levels of $E_p(N_2)$, but the values for $E_p(CO_2)$ were comparable. These results suggest that it was the amine type, whether sterically hindered or unhindered, rather than the small differences in basicity and microstructure that played the greater role in CO_2 permeation barriers across these amine-functionalized membranes. Furthermore, the relationships between CO_2 permeation potential and CO_2/N_2 separation potential via the relationships of $E_p(CO_2)$ vs. $E_p(CO_2) - E_p(N_2)$ are also compared in Figure 18, as plotted in previous studies [40,41]. Lower values are always desired for both $E_p(CO_2)$ and. $E_p(CO_2) - E_p(N_2)$ to in order to attain high performance for CO_2/N_2 separation (the preferred region shown in Figure 19). Obviously, the membranes with hindered amines showed a greater potential to approach the preferred region with both lower $E_p(CO_2)$ and lower $E_p(CO_2) - E_p(N_2)$, and thus could probably attain higher separation performance than membranes with unhindered amines. It is worth noting that amine-free silica membranes generally demonstrate scattered results for CO_2/N_2 separation performance due to the difficulty in precisely controlling pore size, as well as to possible defects induced by a moderate-to-high porous microstructure. The nonporous microstructures of amine-functionalized organosilica membranes, however, lead to a shift in the gas

separation mechanism from one that predominantly exerts a molecular sieving effect of microporous SiO_2 membranes to one that relies on a solution-diffusion (or adsorption-diffusion) model. Thus, these membranes demonstrate great potential in improving CO_2/N_2 separation performance due to the significant increases in CO_2 sorption performance that may highlight differences in the apparent diffusion barriers between CO_2 and N_2 [$E_p(CO_2) - E_p(N_2)$]. In addition, as shown in Figure 19, CO_2 separation membranes can sometimes be designed and prepared prior to a rough preselection of materials, regardless of membrane preparation technique, due to the following possible relationships presented in Equation (10).

$$E_p(CO_2) - E_p(N_2) \approx E_d(CO_2) - E_d(N_2) + \Delta H_s(CO_2) - \Delta H_s(N_2) \equiv \Delta H_s(CO_2)_{eff}, \quad (10)$$

where both $E_d(CO_2) - E_d(N_2)$ and $\Delta H_s(N_2)$ can be reasonably ignored sometimes due to the comparable size of CO_2 and N_2, as well as to the negligible adsorption heat of N_2. In such cases, therefore, the values of $E_p(CO_2) - E_p(N_2)$ can be roughly predicted from the effective adsorption heat of CO_2, $\Delta H_s(CO_2)_{eff}$, which can be fairly measured based on the reversible adsorption/desorption of CO_2 on solid powders, as demonstrated in Figures 10 and 11. Generally, the reversible adsorption amount and heat may vary with the temperature and pressure employed. Therefore, future studies for the systematic and quantitative assessment of $\Delta H_s(CO_2)_{eff}$ are needed. It is worth noting that the membrane microstructure (e.g., pore size or free volume, porosity) also plays an important role in activation energies for gas permeation. Notwithstanding, the relationships shown in Figure 18 makes sense when the comparable microstructures of membranes are considered.

Table 5. Values for E_p and CO_2/N_2 separation performance at 35 °C for amine-functionalized organosilica membranes. Results were reorganized from refs. [21,22].

Membranes	Activation Energies (E_p), [kJ/mol]			Membrane Performance at 35 °C	
	$E_p(CO_2)$	$E_p(N_2)$	$E_p(CO_2) - E_p(N_2)$	CO_2 Permeance [10^{-10} mol/(m² s Pa)]	CO_2/N_2 Ideal Selectivity [-]
PA-Si	8.8	18.0	−9.2	260	22
SA-Si	9.8	16.1	−6.3	170	11
TA-Si	0.2	10.0	−9.8	1720	21
BTPP	9.0	20.4	−11.4	337	25

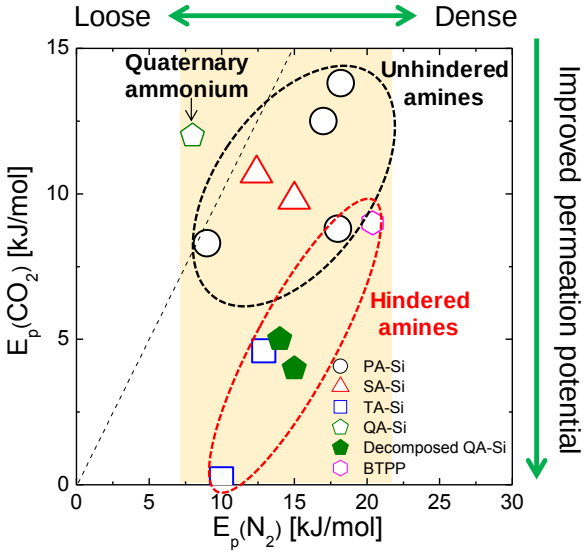

Figure 18. Relationships of $E_p(N_2)$ vs. $E_p(CO_2)$ for amine-functionalized organosilica membranes. Results were reorganized from refs. [21–23].

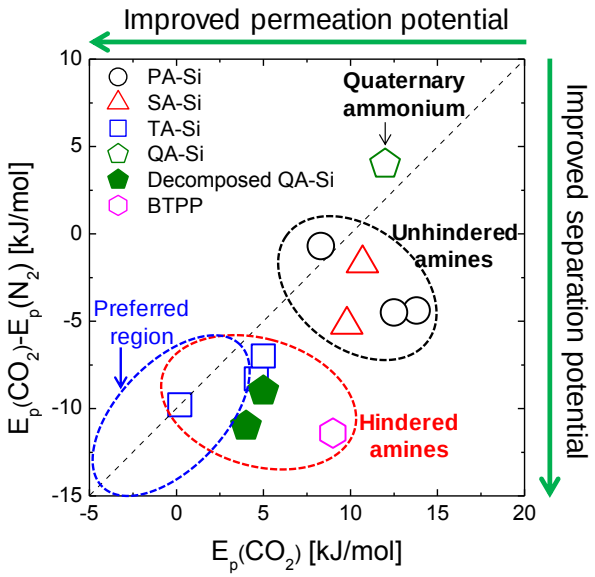

Figure 19. Relationships of $E_P(CO_2)$ vs. $E_P(CO_2) - E_P(N_2)$ for amine-functionalized organosilica membranes. The preferred region shown in the figure demonstrates lower values for both $E_P(CO_2)$ and $E_P(CO_2) - E_P(N_2)$. Results were reorganized from refs. [21–23].

5. Final Remarks and Outlook

This review examines the role of amine type in the CO_2 transport behaviors through amine-functionalized silica/organosilica membranes. Based on a simple summary of reported studies in this field and on a systematic comparison of our previous studies, the term "membrane affinity" is likely to be regarded in a broad sense that comprises not only the favorable interactions of CO_2 molecules with the membrane matrix, but also their promoted/inhibited diffusion within the membrane matrix and from the interface of the membrane permeate side. Hence, the best solutions to synthesize CO_2 separation membranes with high CO_2 transport efficiency should include an optimization of the kinetics of both the sorption and diffusion processes for CO_2. Under mild conditions such as ambient or sub-ambient temperatures, and in the case of comparable membrane microstructures, membranes with hindered amines seem to be the best choice to achieve a good balance between sorption and diffusion processes for CO_2 molecules due to the low-to-moderate CO_2 binding energies that may improve the CO_2 mobility in a membrane matrix. However, more in-depth studies are needed to evaluate the roles of membrane affinity and/or amine type as well as their synergistic effect with the geometrical microstructures of membrane matrices in CO_2 separation performance. In addition, more studies should also be devoted to how temperature affects the amine-CO_2 interactions (or CO_2 mobility in the membrane matrix) to achieve a comprehensive understanding of the role of amine type in CO_2 transport behaviors in both single and mixed gas systems. Studies on the thermal stability of amine groups, relationships between the accessibility of amine groups, and on the microstructures of membranes are also of importance and significance to direct the preparation of high-efficiency CO_2 separation membranes.

Author Contributions: L.Y. wrote the manuscript in consultation with T.T. All authors discussed the results and commented on the manuscript.

Funding: A part of this research was supported by JSPS KAKENHI Grant Numbers JP15H02313 and JP18H03855.

Acknowledgments: L.Y. sincerely acknowledges financial support from the Special Postdoctoral Researcher Program provided by the Global Career Design Center, Hiroshima University. Authors thank for the financial support from JSPS KAKENHI Grant Numbers JP15H02313 and JP18H03855.

Conflicts of Interest: The authors declare no conflict of interest.

References

1. Gin, D.L.; Noble, R.D. Designing the next generation of chemical separation membranes. *Science* **2011**, *332*, 674–676.
2. Car, A.; Stropnik, C.; Yave, W.; Peinemann, K.V. Tailor-made polymeric membranes based on segmented block copolymers for CO_2 separation. *Adv. Funct. Mater.* **2008**, *18*, 2815–2823.
3. He, W.; Wang, Z.; Li, W.; Li, S.; Bai, Z.; Wang, J.; Wang, S. Cyclic tertiary amino group containing fixed carrier membranes for CO_2 separation. *J. Membr. Sci.* **2015**, *476*, 171–181.
4. Chung, T.-S.; Jiang, L.Y.; Li, Y.; Kulprathipanja, S. Mixed matrix membranes (mmms) comprising organic polymers with dispersed inorganic fillers for gas separation. *Prog. Polym. Sci.* **2007**, *32*, 483–507.
5. Hillock, A.M.; Koros, W.J. Cross-linkable polyimide membrane for natural gas purification and carbon dioxide plasticization reduction. *Macromolecules* **2007**, *40*, 583–587.
6. Xomeritakis, G.; Tsai, C.-Y.; Brinker, C.J. Microporous sol–gel derived aminosilicate membrane for enhanced carbon dioxide separation. *Sep. Purif. Technol.* **2005**, *42*, 249–257.
7. Paradis, G.G.; Kreiter, R.; van Tuel, M.M.; Nijmeijer, A.; Vente, J.F. Amino-functionalized microporous hybrid silica membranes. *J. Mater. Chem.* **2012**, *22*, 7258–7264.
8. Suzuki, S.; Messaoud, S.B.; Takagaki, A.; Sugawara, T.; Kikuchi, R.; Oyama, S.T. Development of inorganic–organic hybrid membranes for carbon dioxide/methane separation. *J. Membr. Sci.* **2014**, *471*, 402–411.
9. Jang, K.-S.; Kim, H.-J.; Johnson, J.; Kim, W.-G.; Koros, W.J.; Jones, C.W.; Nair, S. Modified mesoporous silica gas separation membranes on polymeric hollow fibers. *Chem. Mater.* **2011**, *23*, 3025–3028.
10. Messaoud, S.B.; Takagaki, A.; Sugawara, T.; Kikuchi, R.; Oyama, S.T. Alkylamine–silica hybrid membranes for carbon dioxide/methane separation. *J. Membr. Sci.* **2015**, *477*, 161–171.
11. Ostwal, M.; Singh, R.P.; Dec, S.F.; Lusk, M.T.; Way, J.D. 3-aminopropyltriethoxysilane functionalized inorganic membranes for high temperature CO_2/N_2 separation. *J. Membr. Sci.* **2011**, *369*, 139–147.
12. Sakamoto, Y.; Nagata, K.; Yogo, K.; Yamada, K. Preparation and CO_2 separation properties of amine-modified mesoporous silica membranes. *Microporous Mesoporous Mat.* **2007**, *101*, 303–311.
13. Kim, H.-J.; Chaikittisilp, W.; Jang, K.-S.; Didas, S.A.; Johnson, J.R.; Koros, W.J.; Nair, S.; Jones, C.W. Aziridine-functionalized mesoporous silica membranes on polymeric hollow fibers: Synthesis and single-component CO_2 and N_2 permeation properties. *Ind. Eng. Chem. Res.* **2014**, *54*, 4407–4413.
14. Sartori, G.; Ho, W.; Savage, D.; Chludzinski, G.; Wlechert, S. Sterically-hindered amines for acid-gas absorption. *Sep. Purif. Methods* **1987**, *16*, 171–200.
15. Chowdhury, F.A.; Okabe, H.; Yamada, H.; Onoda, M.; Fujioka, Y. Synthesis and selection of hindered new amine absorbents for CO_2 capture. *Energy Procedia* **2011**, *4*, 201–208.
16. Idris, Z.; Eimer, D.A. Representation of CO_2 absorption in sterically hindered amines. *Energy Procedia* **2014**, *51*, 247–252.
17. Chowdhury, F.A.; Yamada, H.; Higashii, T.; Goto, K.; Onoda, M. CO_2 capture by tertiary amine absorbents: A performance comparison study. *Ind. Eng. Chem. Res.* **2013**, *52*, 8323–8331.
18. Zhao, Y.; Ho, W.W. Steric hindrance effect on amine demonstrated in solid polymer membranes for CO_2 transport. *J. Membr. Sci.* **2012**, *415*, 132–138.
19. Zhao, Y.; Ho, W.W. CO_2-selective membranes containing sterically hindered amines for CO_2/H_2 separation. *Ind. Eng. Chem. Res.* **2012**, *52*, 8774–8782.
20. Tong, Z.; Ho, W.W. New sterically hindered polyvinylamine membranes for CO_2 separation and capture. *J. Membr. Sci.* **2017**, *543*, 202–211.
21. Yu, L.; Kanezashi, M.; Nagasawa, H.; Oshita, J.; Naka, A.; Tsuru, T. Pyrimidine-bridged organoalkoxysilane membrane for high-efficiency CO_2 transport via mild affinity. *Sep. Purif. Technol.* **2017**, *178*, 232–241.
22. Yu, L.; Kanezashi, M.; Nagasawa, H.; Tsuru, T. Fabrication and CO_2 permeation properties of amine-silica membranes using a variety of amine types. *J. Membr. Sci.* **2017**, *541*, 447–456.
23. Yu, L.; Kanezashi, M.; Nagasawa, H.; Moriyama, N.; Tsuru, T.; Ito, K. Enhanced CO_2 separation performance for tertiary amine-silica membranes via thermally induced local liberation of CH_3Cl. *AIChE J.* **2018**, *64*, 1528–1539.
24. Yu, L.; Kanezashi, M.; Nagasawa, H.; Ohshita, J.; Naka, A.; Tsuru, T. Fabrication and microstructure tuning of a pyrimidine-bridged organoalkoxysilane membrane for CO_2 separation. *Ind. Eng. Chem. Res.* **2017**, *56*, 1316–1326.

25. Pera-Titus, M. Porous inorganic membranes for CO_2 capture: Present and prospects. *Chem. Rev.* **2013**, *114*, 1413–1492.
26. Caplow, M. Kinetics of carbamate formation and breakdown. *J. Am. Chem. Soc.* **1968**, *90*, 6795–6803.
27. Li, Y.; Wang, S.; He, G.; Wu, H.; Pan, F.; Jiang, Z. Facilitated transport of small molecules and ions for energy-efficient membranes. *Chem. Soc. Rev.* **2015**, *44*, 103–118.
28. Donaldson, T.L.; Nguyen, Y.N. Carbon dioxide reaction kinetics and transport in aqueous amine membranes. *Ind. Eng. Chem. Fund.* **1980**, *19*, 260–266.
29. Sartori, G.; Savage, D.W. Sterically hindered amines for carbon dioxide removal from gases. *Ind. Eng. Chem. Fund.* **1983**, *22*, 239–249.
30. Xomeritakis, G.; Tsai, C.; Jiang, Y.; Brinker, C. Tubular ceramic-supported sol–gel silica-based membranes for flue gas carbon dioxide capture and sequestration. *J. Membr. Sci.* **2009**, *341*, 30–36.
31. Kim, H.-J.; Yang, H.-C.; Chung, D.-Y.; Yang, I.-H.; Choi, Y.J.; Moon, J.-k. Functionalized mesoporous silica membranes for CO_2 separation applications. *J. Chem.* **2015**, *2015*.
32. Kanezashi, M.; Matsugasako, R.; Tawarayama, H.; Nagasawa, H.; Yoshioka, T.; Tsuru, T. Tuning the pore sizes of novel silica membranes for improved gas permeation properties via an in situ reaction between NH_3 and Si–H groups. *Chem. Commun.* **2015**, *51*, 2551–2554.
33. Miyamoto, M.; Takayama, A.; Uemiya, S.; Yogo, K. Gas permeation properties of amine loaded mesoporous silica membranes for CO_2 separation. *Desalin. Water Treat.* **2011**, *34*, 266–271.
34. Merkel, T.C.; Lin, H.; Wei, X.; Baker, R. Power plant post-combustion carbon dioxide capture: An opportunity for membranes. *J. Membr. Sci.* **2010**, *359*, 126–139.
35. Gouedard, C.; Picq, D.; Launay, F.; Carrette, P.-L. Amine degradation in CO_2 capture. I. A review. *Int. J. Greenh. Gas Control* **2012**, *10*, 244–270.
36. Ren, X.; Nishimoto, K.; Kanezashi, M.; Nagasawa, H.; Yoshioka, T.; Tsuru, T. CO_2 permeation through hybrid organosilica membranes in the presence of water vapor. *Ind. Eng. Chem. Res.* **2014**, *53*, 6113–6120.
37. Hahn, M.W.; Jelic, J.; Berger, E.; Reuter, K.; Jentys, A.; Lercher, J.A. Role of amine functionality for CO_2 chemisorption on silica. *J. Phys. Chem. B* **2016**, *120*, 1988–1995.
38. Kim, Y.E.; Lim, J.A.; Jeong, S.K.; Yoon, Y.I.; Bae, S.T.; Nam, S.C. Comparison of carbon dioxide absorption in aqueous mea, dea, tea, and amp solutions. *Bull. Korean Chem. Soc.* **2013**, *34*, 783–787.
39. Van Amerongen, G.J. The permeability of different rubbers to gases and its relation to diffusivity and solubility. *J. Appl. Phys.* **1946**, *17*, 972–985.
40. Koros, W.J. *Barrier Polymers and Structures*; ACS Publications: Washington, DC, USA, 1990.
41. Singh-Ghosal, A.; Koros, W. Energetic and entropic contributions to mobility selectivity in glassy polymers for gas separation membranes. *Ind. Eng. Chem. Res.* **1999**, *38*, 3647–3654.
42. Fu, S.; Sanders, E.S.; Kulkarni, S.S.; Wenz, G.B.; Koros, W.J. Temperature dependence of gas transport and sorption in carbon molecular sieve membranes derived from four 6fda based polyimides: Entropic selectivity evaluation. *Carbon* **2015**, *95*, 995–1006.
43. Du, N.; Park, H.B.; Robertson, G.P.; Dal-Cin, M.M.; Visser, T.; Scoles, L.; Guiver, M.D. Polymer nanosieve membranes for CO_2-capture applications. *Nat. Mater.* **2011**, *10*, 372–375.